between Austenitic Stainless Steel **(**ASS) and Ferritic Stainless Steel **(**FSS) is usually carried out by GTAW with type 309 SS filler to avoid formation of hard and brittle martensite and to produce a ductile austenitic weld metal (WM). However, the problem of extensive grain coarsening on FSS side, due to its higher diffusivity, cannot be avoided. The problem becomes more acute in thin sheet DMW, where no filler can be used.

The present micro structural study had been undertaken with the objective to produce ductile autogeneous laser butt weld between type 304 ASS and stabilized 17% Cr ferritic SS. The microstructure of WM was favorably engineered by preferential displacement of focused laser beam towards ASS side. LW effectively reduced the extent of heat-affected zone, especially in ferritic SS. In contrast to coarse-grained micro-structure of the autogeneous GTA weld with large blocks of ferrite and martensite/retained austenite, LW produce highly refined microstructure in the WM. Largely austenitic WM was achieved by the use of nitrogen as the shroud gas. Fig. L.13.1 shows change in WM microstructure with different welding parameters. [R. Kaul, P. Ganesh and A. K. Nath, J. of Laser Applications 17(1), 2005].

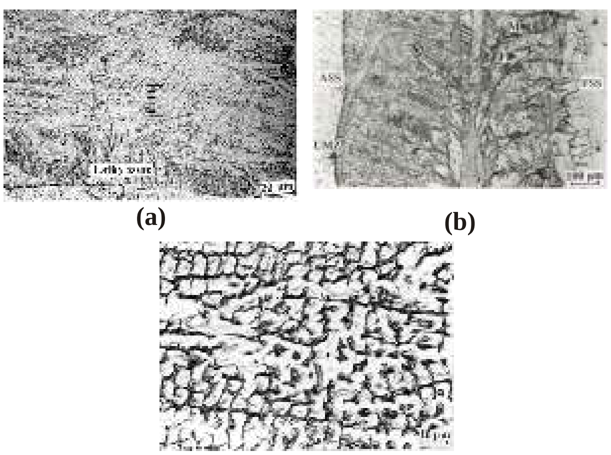

(a) **(b)**

(c)

Fig L.13.1 *Microstructure of LWM produced by, (a) focused laser beam at the center, (b) preferentially displaced focused laser beam towards ASS side (c) preferentially displaced focused laser beam towards ASS side with nitrogen as the shroud gas*

(Contributed by: A.K. Nath; aknath@cat.ernet.in)

L.14 Laser Rapid Manufacturing

Laser rapid manufacturing (LRM) is a new class of technology used for fabricating engineering components by direct deposition of metal powder according to 3D computer-aided design (CAD) data. Unlike CNC machines tools, which are subtractive in nature, RM systems fuse together metal powder to form complex parts. This is basically an extension of the laser cladding to three-dimensional deposition and a promising technology for low volume manufacturing.

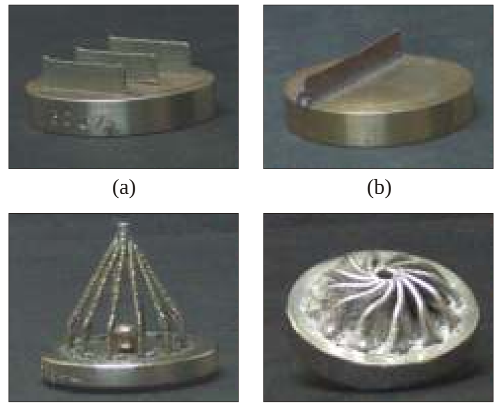

(a) (b)

(c) (d)

Fig L.14 (a) SS316L walls of different thickness (0.8-1.2mm) on SS304L substrate, (b) Cu wall over SS304L substrate, (c) Cage and (d) Impeller

A LRM facility has been set up integrating the indigenously developed 3.5kW CW CO_2 laser with an in-house developed co-axial powder feeding system and a 5-axis CNC machine. The powder feeder can feed the SS316L metal powder from 2 g/min to 30 g/min with a 0.2g/min increment. A number engineering components of simple geometry have been fabricated, using SS316L, Inconel-625, Colmonoy-6, Cu powders over SS304L substrate. The fabricated components have dimensional accuracy about 100 microns and surface finish 5-7 Ra value for SS316L material. LRM deposited material has demonstrated high tensile properties with low ductility for SS316L and Inconel-625.

(Contributed by: A.K. Nath; aknath@cat.ernet.in)

L.15 Quest for magnetic materials for newer technology

We are carrying out detailed experimental work (e.g., magnetization, magnetotransport, etc.) on the intermetallic compound Gd_5Ge_4 probing the FOMST and the different magnetic phases in the compound.

Gd_5Ge_4 is the parent compound of the $Gd_5(Ge_{1-x}Si_x)_4$ series. This series of compounds is under intense experimental study worldwide, in connection with the phenomena of giant magnetocaloric effect, giant magnetoresistance, and colossal magnetostriction. All these phenomena are due to simultaneous magnetic and crystallographic (Martensitic) transformations induced by H and temperature (T). Gd_5Ge_4 orders antiferromagnetically at T_N » 130 K, and in H lower than 10 kOe, the antiferromagnetic (AFM) order is sustained at least down to 2K. Under applied H exceeding 10 kOe (the precise H value is T-dependent), Gd_5Ge_4 shows interesting AFM to ferromagnetic (FM) transition that could be driven both by T and H.

Isothermal magnetization and magnetic relaxation measurements in polycrystalline Gd_5Ge_4 were carried. The results show that upon field variation from the initial ZFC state the magnetic-field-induced first order AFM to FM transition observed in Gd_5Ge_4 is accompanied by distinct metastability. The reverse transition from the FM state to AFM state on reducing H is also marked with same kind of metastability in the temperature region above 21 K. Below 21 K, this FM to AFM transition process is hindered. At 5 K, the sample remains in the FM state at all fields including zero field after it has been magnetized at H > 25 kOe. This FM state is sustained on subsequent field cycling between ± 50 kOe. At 15K, the FM to AFM transition is initiated in the descending-H cycle but remains incomplete even when the magnetic field is reduced to zero. This leads to the interesting situation of phase-coexistence between the converted stable AFM state and the unconverted FM state, which is also stable within the

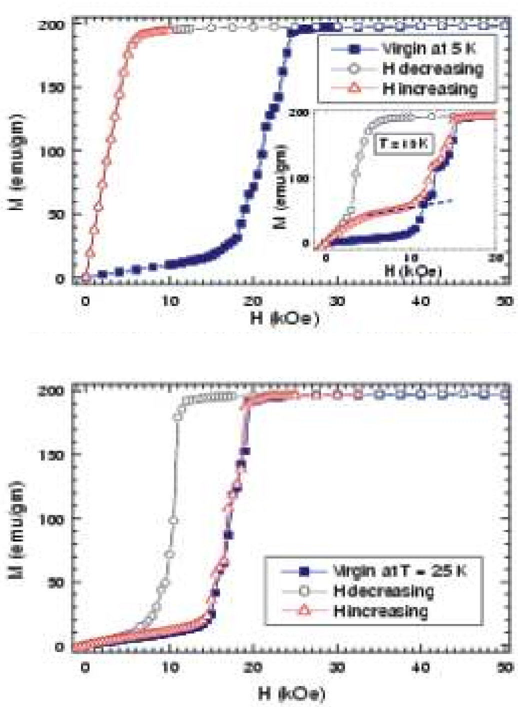

Fig L.15.1 *Isothermal H dependence of magnetization of polycrystalline Gd_5Ge_4 highlighting fully arrested, partially arrested, and de-arrested FM phases at different T values*

experimental time scale. This phase-coexistence is different from the phase-coexistence observed across the AFM to FM transition in the virgin sample both below and above 21 K, and across the FM to AFM transition in the isothermal descending-H cycle above 21 K. Here, one of the phases- the AFM phase during the virgin cycle and the FM phase in the H descending cycle- is metastable and relaxes towards the stable phase because of fluctuation energies. These results have been published recently [M. K. Chattopadhyay et al. Phys. Rev. B 70 (2004) 214421].

Detailed magnetotransport and magnetization studies on Gd_5Ge_4 are in progress. These studies have already lead to very new findings, viz., presence of spin fluctuations within the stable AF state, important aspects regarding the dynamics of phase transition in phase separated systems in the presence of magneto-structural coupling, etc. We believe that all these efforts would lead to significant inputs towards finding newer technology for tuning materials suitable for the machines of the future years.

(Contributed by: M. K. Chattopadhyay (maulindu@cat.ernet.in) and Meghmalhar Manekar)

L.16 Development of lithium niobate crystal elements

Non-linear and photorefractive crystals are suitable candidates for many optical applications, e.g. laser output modifications, optical signal amplification, phase conjugation, image processing, reversible holographic storage, all solid state UV laser, and compact blue green laser systems. For many years the ferroelectric lithium niobate has been of great interest for both fundamental science and application because of its unique combination of electro-optic, piezoelectric, non-linear optical properties with nonhygroscopic, mechanical and chemical stability. The typical applications of lithium niobate are non-linear frequency conversions, parametric light generation and amplifications, electro-optical modulators, wave guide structures, acoustic wave delay lines acoustic filters, non-volatile holographic data storage, domain engineering, QPM based compact green micro-laser systems and display devices. Applications that utilize the large electro-optic coefficients of lithium niobate are optical modulation and Q-switching of infrared wavelengths. Applications that use the large nonlinear d coefficient of $LiNbO_3$ (LN) include optical parametric oscillation, difference frequency mixing to generate tunable infrared wavelengths and second harmonic generation. The periodically poled lithium niobate crystals are particularly attractive for second harmonic generation of low power laser diodes in the 1.3 - 1.55µm range